Aperture of rough cracks

Franck Plouraboué, Pascal Kurowski, Jean-Pierre Hulin, and Stéphane Roux
Laboratoire de Physique et Mécanique des Milieux Hétérogènes, Ecole Supérieure de Physique et Chimie Industrielles, 10 rue Vauquelin, 75231 Paris Cedex 05, France

Jean Schmittbuhl
Laboratoire de Géophysique, Ecole Normale Supérieure, 24 rue Lhomond, 75231 Paris Cedex 05, France
(Received 18 July 1994)

We analyze the problem of the geometrical aperture between the two faces of a crack described as a self-affine surface. We consider the contact of the two surfaces after a relative rigid-body displacement (translation and/or rotation) of one side of the crack with respect to the opposite one. A number of properties are obtained analytically and illustrated by numerical simulations on generated self-affine surfaces. The results concern the scaling of the average aperture, which is shown to include a very slowly varying correction term (logarithmic with respect to the displacement); this affects severely the dependence of the measured aperture on the displacement. These results are used to analyze experimental data obtained on a granite sample and to estimate the roughness exponent from a global measurement. This estimate is shown to agree with an analysis of the roughness based on profilometry measurements.

PACS number(s): 02.50.−r, 47.55.Mh, 47.53.+n, 62.20.Mk

I. INTRODUCTION

The transport properties of fractured materials is a topic of very broad practical relevance in many domains such as hydrology, civil and petroleum engineering, geothermal processes, and chemical and nuclear waste disposal [1]. In the particular example of geothermics, heat is extracted from fractured hot deep rocks by forcing a fluid circulation between two boreholes. It is thus a fundamental interest to understand the flow properties in the cracks and more generally in the fracture network in order to model the heat production. Some of the phenomena occur at the scale of the fracture network and involve the understanding of its connectivity, which may involve a very complex and structured array of cracks (see, e.g., Refs. [2,3]) and of the influence of the distribution of apertures [4]; however, a good understanding of the structure and transport properties of *individual* fractures [5] is mandatory to model satisfactorily the global system.

A first key parameter is the fracture aperture which determines partly the fracture permeability. For instance, Witherspoon [6] and Brown [7] have studied the relevance of the so-called "cubic law," which gives the scaling of the hydraulic conductance with the aperture of a crack with a rough boundary. Another important parameter is the roughness of the fracture walls which will strongly influence the structure of the flow field inside the fracture. Solving the flow field past a rough boundary is a problem which has been addressed recently by Gutfreund and Hansen [8] using a lattice-gas algorithm in two dimensions. These studies reveal the importance of an accurate description of the geometry of the crack so as to determine the hydraulic flow properties.

In Refs. [7,8], the geometry of the boundaries was considered as being described by self-affine surfaces or profiles. Such a geometry is well suited for describing crack surfaces. Indeed, a self-affine geometry [9] has been evidenced in many cracks, with various materials, loading models, fracturing conditions, and sample sizes (see, e.g., Refs. [10–15] and references therein). Such a statistical description accounts accurately for the size effects in crack roughness; in particular, it leads to predictions at the field scale from laboratory experiments through scaling arguments. Many previous experiments have concentrated on the identification of the self-affine geometry of fracture surfaces, using local measurements such as surface profilometry or image analysis techniques.

However, very frequently, the two facing sides of a crack in a fractured block of material will be displaced relative to each other. This displacement prevents the two halves of the block from coming again in contact after the fracturing stress is released; the effective aperture is then essentially controlled by the roughness and by the relative displacement. In the present paper, we analyze how the macroscopic effective aperture of a fracture is related to its microscopic structure and in particular to the relative displacement of the two facing sides of the crack.

In this particular case, determining the aperture reduces to a problem of geometry using the statistical features of self-affine surfaces. The physical implications of the results presented below are numerous. We have already motivated our study by the importance of flow in open cracks for geophysics. We could have equally well mentioned the problem of the mechanical behavior of a rock joint. In the latter case, the aperture will allow the determination of some crucial parameters for the macroscopic friction, such as the dilation angle (derivative of the aperture with respect to the relative parallel displacement). Size effects that are well documented from experiments and practice are essentially phenomenologically

described in most cases (see in particular Ref. [16] for a broad review on these problems.) The existence of long-range correlations in the surface topography and in particular the self-affine nature of the crack geometry may be partly responsible for those size effects. However, in order to base those speculations on a firm ground it is essential to characterize properly the statistical properties of the aperture between two conjugated rough surfaces. This question is the heart of the present study.

We shall first discuss, using scaling arguments, which type of relation is to be expected between the aperture and the lateral displacement of the crack surfaces. We will also discuss the case of rotations. We shall then attempt to verify these predictions through the numerical simulations on computer generated rough surfaces and on laboratory experiments on a fractured granite block.

II. SELF-AFFINE FRACTURE SURFACES

Let us first introduce a few basic properties of such rough surfaces, so that we can derive an analytic expression of the aperture in the following section. A surface is said to be self-affine [9] when it satisfies a scale invariance with different dilation ratios along different space directions, more precisely, if the surface is *statistically* unchanged under the rescaling

$$x \rightarrow \lambda_1 x \ , \quad y \rightarrow \lambda_2 y \ , \quad z \rightarrow \lambda_3 z \ , \tag{1}$$

where all different dilation ratios λ_i are functions of only one of them, say λ_1, chosen as a reference. Moreover, since a group property is required for these transformations, the dependence of λ_i $(i=2,3)$ on λ_1 is through a homogeneous function. This implies the existence of two independent scaling exponents ζ_i for $i=2$ and 3 such that

$$\lambda_i = \lambda_1^{\zeta_i} \ . \tag{2}$$

For a crack in three dimensions, we chose directions x and y located in the mean plane of the fracture. Ignoring overhangs, which is legitimate for crack surfaces, the surface is represented by a single valued function $z(x,y)$. Although it is not intuitively obvious, various topographical measurements have revealed that x and y play similar roles and thus $\zeta_2=\zeta_3$ for very different materials including rocks. In the following, we will restrict our discussions to such isotropic—in the (x,y) plane—surfaces and thus we will call ζ the common value of the two scaling exponents. Figure 1 shows a synthetic self-affine surface characterized by a roughness exponent equal to $\zeta=0.83$, comparable to the typical value observed for cracks, and chosen to match precisely the value measured in the experiment detailed below.

Let us now use this scale invariance to express some properties of the surface topography. As the (x,y) plane represents the mean plane of the surface, we have $\langle z(x,y)\rangle=0$. An interesting parameter is the spatial correlation

$$C(u)=\langle (z(x,y)-z(x+u,y))^2 \rangle \ , \tag{3}$$

where the average $\langle\ \rangle$ is taken over x and y. We have considered above the correlation along the x direction, although this choice is not restrictive, since x and y are considered as equivalent (isotropic surface). The function $C(u)$ must fulfill the prescribed invariance relation (1) and hence $C(\lambda u)=\lambda^{2\zeta}C(u)$ (for positive λ) or

$$C(u)=C(l)\left|\frac{u}{l}\right|^{2\zeta} , \tag{4}$$

where l is an arbitrary microscopic length scale. From now on we will implicitly assume that u is positive, unless explicitly stated. The symmetry $u \rightarrow -u$ is a simple consequence of the isotropy of the surface in its mean plane. Expanding the expression of $C(u)$ [Eq. (3)] leads to an equivalent form

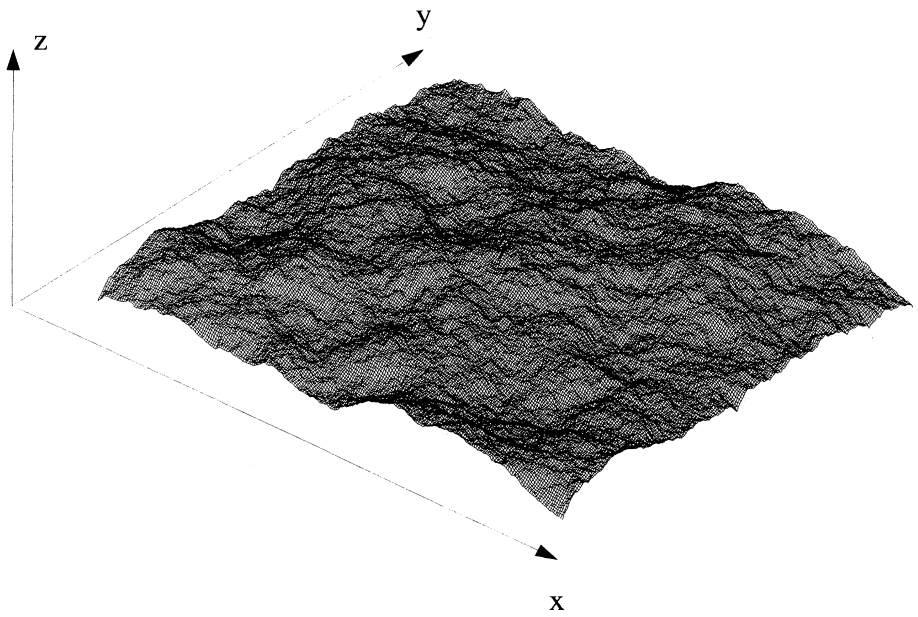

FIG. 1. Example of a self-affine surface with an exponent $\zeta=0.83$ and a size $L=256$.

$$\frac{\langle z(x,y)z(x+u,y)\rangle}{\langle z(x,y)^2\rangle}=1-A^2\left[\frac{u}{l}\right]^{2\zeta}, \tag{5}$$

where

$$A^2=\frac{C(l)}{2\langle z(x,y)^2\rangle}. \tag{6}$$

A is independent of the distance u, but it does depend on other parameters of the surface. Indeed, the variance of the height $\sigma^2=\langle z(x,y)^2\rangle$ must depend on the size of the surface, assuming that the short-scale features are kept constant as the system size is varied. For a surface that extends over $0<x<L$ and $0<y<L$, again using the scale invariance (1) provides $\sigma^2\propto L^{2\zeta}$ and thus

$$A\propto L^{-\zeta}. \tag{7}$$

Moreover, it should be kept in mind that albeit the mathematical concept of scale invariance does not allow for cutoffs, any natural system will only display such a symmetry over a limited range of length scales whose limits will be referred to as the lower and upper cutoff length scales. For the case of fractures, the lower cutoff may be given by the scale at which the microstructure of the material becomes apparent (i.e., grain or pore size, etc.). However, for the granite rock studied and discussed in Sec. X, the scale invariance seems to hold even down to scales smaller than the maximum grain size of the microstructure and hence the apparent lower limit is given by the precision of the measurements. Experimentally, it appears that an upper cutoff is seldomly observed and, in most cases, the scaling extends over the entire system size (once bias arising from the method of determination of the self-affine character has been considered).

III. APERTURE CORRELATIONS

Let us first analyze the case of two *statistically independent* surfaces $z_1(x,y)$ and $z_2(x,y)$ with the same roughness exponent ζ and facing each other. The distance between the two surfaces $a(x,y)=z_2(x,y)-z_1(x,y)$ is again a self-affine function with the same value of ζ, even if the mean amplitudes of the roughness of z_1 and z_2 are different.

We can also mention here the case where the two roughness exponents of the surfaces are different. Let us call ζ_1 and ζ_2 the roughness exponents and $C_1(l)$ and $C_2(l)$ the amplitudes as introduced in Eqs. (3) and (4). There exists a well-defined scale Δx^* for which the roughness of the two surfaces are of the same magnitude $C_1(\Delta x^*)=C_2(\Delta x^*)$. Using Eq. (4), we can rewrite the latter condition as

$$\sqrt{C_1(l)}\left[\frac{\Delta x^*}{l}\right]^{\zeta_1}=\sqrt{C_2(l)}\left[\frac{\Delta x^*}{l}\right]^{\zeta_2}. \tag{8}$$

Above the scale Δx^*, the distance $a(x,y)$ is a self-affine function characterized by a roughness exponent $\zeta=\max(\zeta_1,\zeta_2)$. On the contrary, at scales lower than Δx^*, a is also self-affine but with an exponent equal to $\zeta=\min(\zeta_1,\zeta_2)$. We assumed here that the crossover scale is in the range where both surfaces can be considered as self-affine. Otherwise, only one of the two regimes mentioned above is observed depending on the position of Δx^* compared to the upper or lower cutoff scales for both surfaces.

The previous results hold for the case of two independent surfaces describing the structure of the fracture aperture at very small length scales. Let us now handle a more complex case, namely, the case where z_1 and z_2 are strongly correlated, because one is simply obtained from the other by a translation along x.

Let us first discuss qualitatively the spatial correlation of the aperture variation between the two facing sides of the crack when they are displaced by a distance u. At length scales v smaller than the displacement u, the height variations of the two facing surfaces are statistically independent. Indeed, observing the aperture over a window of size smaller than the displacement does not allow one to detect the correlations between them and thus one can use the result obtained for independent self-affine surfaces.

On the contrary, when the observation scale v is much larger than the initial displacement, the similarity between the two facing surfaces becomes apparent. If we imagine the effect of adding a harmonic modulation to the surface with an amplitude A and a wave-length λ large compared to the displacement u, both sides of the crack are subject to the same modulation and the effect of this perturbation on the aperture can be estimated to Au/λ, which vanishes with the ratio u/λ. For a self-affine surface, the amplitude on average increases with the wavelength, but slower than λ, so that the dominant contribution to the aperture essentially comes from wavelengths of order u. Therefore, at these larger length scales, the aperture is no longer self-affine but tends to be uncorrelated. Let us now turn to a quantitative analysis of the aperture.

Let us consider a crack that has been subjected to a slip u along the x axis and h along the z axis: $z_2(x,y)=z_1(x+u,y)+h$. It will be the subject of Sec. IV to determine the value of h which gives rise to a single contact between the two facing surfaces. In the present section we simply consider h as being a constant and it will not appear in the following discussion. The aperture $a_u(x,y)$ is equal to

$$a_u(x,y)=z(x+u,y)-z(x,y)+h. \tag{9}$$

Using the fact that $\langle z\rangle=0$, we have $\langle a\rangle=h$. Let us now analyze the correlations in the aperture function, through

$$\varphi(v,u)=\langle[a_u(x,y)-a_u(x+v,y)]^2\rangle. \tag{10}$$

Using the definition of the aperture, we can rewrite the function (10) in the following form, which displays a symmetry of this function:

$$\begin{aligned}\varphi(v,u)&=\langle[z(x,y)-z(x+u,y)\\&\quad-z(x+v,y)+z(x+u+v,y)]^2\rangle\\&=\varphi(u,v).\end{aligned} \tag{11}$$

Moreover the self-affinity of the surface results in the

homogeneity property

$$\varphi(\lambda u,\lambda v)=\lambda^{2\zeta}\varphi(u,v)\ . \tag{12}$$

Using this invariance, φ can be determined from a single variable function $\psi(u)=\varphi(u,1)$ with $\varphi(u,v)=v^{2\zeta}\psi(u/v)$. The symmetry of φ implies

$$\psi(u)=u^{2\zeta}\psi(1/u)\ . \tag{13}$$

To obtain the ψ function we expand Eq. (11) and use expressions (3)–(5):

$$\psi(u)=\frac{2C(l)}{l^{2\zeta}}[1+u^{2\zeta}-\tfrac{1}{2}(1+u)^{2\zeta}-\tfrac{1}{2}|1-u|^{2\zeta}]\ . \tag{14}$$

The absolute value in Eq. (14) is similar to the one appearing in Eq. (4) and has been explicitly introduced in this equation so as to describe both cases $u<1$ and $u>1$. This function is shown in Fig. 2 for three values of the exponent $\zeta=0.25$, 0.5, and 0.75. Two limiting behaviors are interesting.

First when $u\ll 1$, a Taylor expansion of ψ gives

$$\psi(u)=\frac{2C(l)}{l^{2\zeta}}[u^{2\zeta}-\zeta(2\zeta-1)u^2]\ . \tag{15}$$

In the usual case $0<\zeta<1$, the leading term is $\psi(u)\propto u^{2\zeta}$.

Second, in the opposite limit where $u\gg 1$, we can resort to Eq. (13) in order to extract the limiting behavior

$$\psi(u)=\frac{2C(l)}{l^{2\zeta}}[1-\zeta(2\zeta-1)u^{(2\zeta-2)}] \tag{16}$$

and hence $\psi(u)$ approaches a constant for large arguments.

From expressions (15) and (16), we deduce the following approximate behavior of φ valid for $v\ll u$ or $v\gg u$:

$$\varphi(u,v)=2C(l)[\min(u/l,v/l)]^{2\zeta}\ . \tag{17}$$

This expression describes correctly the asymptotic behavior $u\ll v$ or $u\gg v$. It is also exact for all values of (u,v) when $\zeta=0.5$. Otherwise, the crossover in the vicinity of $u=v$ is not accurately described.

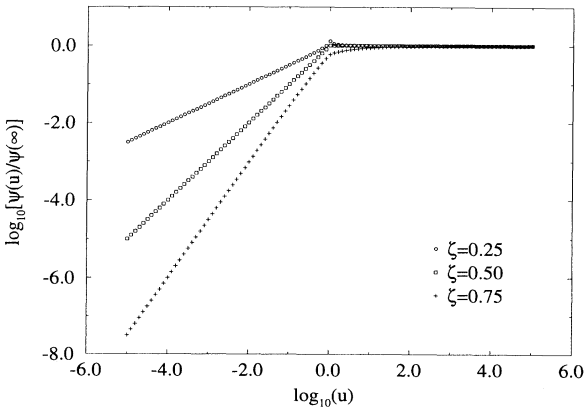

FIG. 2. Analysis of the aperture correlation function expressed through the dimensionless function $\psi(u)/\psi(\infty)$ (see text) as a function expressed through the dimensionless function $\psi(u)/\psi(\infty)$ (see text) as a function of the ratio u between the scale of observation and the displacement between the two surfaces. Three values of the roughness exponent are shown $\zeta=0.25$, 0.50, and 0.75.

The aperture of the crack is self-affine at length scales smaller than the slip u; above this scale, the rms aperture difference is no longer dependent on the distance. In order to be more precise, let us now analyze the correlations in the aperture function. Following similar lines, one can compute the covariance of the aperture at two distant points. This covariance is, by definition,

$$\mathcal{C}(a_u(x,y),a_u(x+v,y))=\frac{\chi(u,v)}{\chi(u,0)}\ , \tag{18}$$

where

$$\chi(u,v)=\langle a_u(x,y)a_u(x+v,y)\rangle - \langle a_u(x,y)\rangle\langle a_u(x+v,y)\rangle\ . \tag{19}$$

A long but easy computation gives

$$\chi(u,v)=\frac{C(l)v^{2\zeta}}{l^{2\zeta}}\left[\left[1+\frac{u}{v}\right]^{2\zeta}+\left|1-\frac{u}{v}\right|^{2\zeta}-2\right]\ . \tag{20}$$

In the limit $v/u\gg 1$, a Taylor expansion provides the asymptotic expression

$$\mathcal{C}(a_u(x,y),a_u(x+v,y))=\zeta(2\zeta-1)\left[\frac{u}{v}\right]^{2(\zeta-1)}\ . \tag{21}$$

Since in our case ζ is smaller than one, the latter expression vanishes as v/u tends to infinity. Thus the aperture at two distant points can be considered as uncorrelated when the distance v is much larger than the displacement u.

IV. EFFECTIVE APERTURE BETWEEN DISPLACED MATCHING ROUGH SURFACES IN CONTACT

In this section we aim at computing the minimum vertical displacement $h(u)$ needed to move the two surfaces by a distance u horizontally while keeping them in contact. At the present stage we only consider rigid translations of two identical surfaces. No rotations are included. The height $h(u)$ to obtain a contact between the surfaces is such that the aperture $a(x,y)$ is always positive and reaches 0 at one point. (The simultaneous occurrence of more than one contact point has a zero probability when rotations are not considered.) Thus

$$h(u)=\max_{(x,y)}(z(x,y)-z(x+u,y)) \tag{22}$$

(assuming that the upper surface has been displaced by a distance u along x).

In order to use the results of Sec. III, we partition the surface into squares S_i of size $u\times u$ so that

$$h_i=\max_{(x,y)\in S_i}(z(x,y)-z(x+u,y))\ , \tag{23a}$$

$$h(u)=\max_i(h_i)\ . \tag{23b}$$

Let us now first estimate the terms h_i. From the previous discussion, the two facing surfaces inside a domain S_i can

be considered as statistically independent. Therefore, the difference $d_u(x,y)=(z(x,y)-z(x+u,y))$ is also self-affine. This implies that the statistical distribution $p_1(d)$ of $d=d_u(x,y)$ should only depend on the reduced variable d/u^{ζ}, so that

$$p_1(d)=u^{-\zeta}\phi_1(d/u^{\zeta}) , \tag{24}$$

where the prefactor comes from the normalization.

To our knowledge, there is no general result about the precise form of ϕ_1. However, in a number of cases, a Gaussian distribution of heights can be argued for. First, it has been found experimentally on fractures [17] that ϕ_1 was accurately described as a Gaussian distribution for low-order moments. Let us also mention that other possibilities exist, such as the recently proposed multifractal nature of the surface [18], which would render the Gaussian statistics only legitimate for low-order moments. This multifractal character, if confirmed, might affect the validity of the proposed analysis and provide another possible explanation for the observed properties reported below. We will see that the simpler assumption of a monofractal self-affine character is sufficient to account for the observed experimental data and the validity of our theoretical analysis is also supported by the numerical simulations on synthetic monofractal self-affine surfaces. We will thus assume from now on that the surface is described by a single roughness exponent (valid for all moments of the height distribution).

Second, known algorithms, such as the one of Voss [19], for generating artificial self-affine profiles also display such a distribution for the height difference when u is large enough, although a Gaussian distribution is not prescribed locally. (Small scale height differences still depend on the details of the numerical procedure.) From now on, we will assume that ϕ_1 can accurately be described by a Gaussian distribution. In the numerical and experimental sections of this paper, we will validate this hypothesis directly.

Using the distribution of d, we have first to compute the statistical distribution $p_2(h)$ of h_i [Eq. (23)]. The main difficulty to obtain p_2 lies in the fact that the different d over which the maximum has to be considered are strongly correlated since $d(x)$ is self-affine.

Some partial results may be found in the literature. Theoretically, Lévy [20] found the probability distribution of the maximum of a random walk starting at the origin (in $1+1$ dimensions). A random walk is a particular example of a self-affine function with a roughness exponent equal to 0.5. The statistical distribution of the maximum over a finite interval is a Gaussian centered in 0 and truncated to positive values. Recent extensions [21] to fractional Brownian motion in $1+1$ dimension (i.e., a more general class of self-affine profile) have been proposed and provide bounds for this distribution.

In fact, we do not need the complete expression of p_2, but rather its behavior for large apertures. In order to get some indications on this limit, we first note that a reduced form similar to Eq. (24) should also hold for the distribution of aperture h_i [Eq. (23)] $p_2(h)=u^{-\zeta}\phi_2(h/u^{\zeta})$. Then, we assume that the large h tail of the distribution ϕ_2 behaves as a Gaussian comparable to ϕ_1

$$\phi_2(h)\sim K\exp\left[-\frac{h^2}{(ku^{\zeta})^2}\right] \tag{25}$$

valid for large h where K and k are two constants. We note that this form is consistent with the above mentioned results on random walks and fractional Brownian motion. This precise form will also be checked directly in Sec. VII.

Finally, from the distribution of h_i, we have to compute the mean value of $h(u)$ from Eq. (23b). In Sec. III we have seen that, above the scale u, the aperture can be considered as an uncorrelated white noise. This means that we can make the approximation that the various h_i are statistically independent. In order to estimate the value of h we resort to a fundamental results of "extreme value statistics" [22], which states that the expectation value h of the maximum among n independent statistical variables picked from the same statistical distribution p_2 fulfills

$$\int_h^{\infty} p_2(h')dh'=1/n . \tag{26}$$

In our case, n is the number of squares S_i in the original surface, or $n=(L/u)^2$. Using the rescaled form of p_2 together with the expression of n, we finally obtain

$$\operatorname{erfc}\left[\frac{h}{ku^{\zeta}}\right]\propto\left[\frac{u}{L}\right]^2 , \tag{27}$$

where erfc is the complementary error function. Using the asymptotic behavior of the complementary error function, we finally arrive at the expression

$$h(u)\propto u^{\zeta}\sqrt{1+K'\ln(L/u)} . \tag{28}$$

In Ref. [23], the above problem was addressed and the aperture was argued to scale as $h(u)\propto u^{\zeta}$, on the basis of a simple scale invariance argument. As shown above, this scaling is expected to be valid for h_i in each box individually. The fact that $h(u)$ is the maximum over a number of such variables which depends on u for fixed L introduces a correction term $[\ln(L/u)]^{1/2}$, which has a significant influence. The magnitude of the correction term is large for small u; however, the slope of $h(u)$ versus u in a log-log plot approaches ζ when u tends to zero because the rate of variation of the correction term is small. A quantitative illustration of this effect is shown in Sec. VII.

V. ROTATIONS AROUND THE z AXIS

Up to now, we have considered a rigid translation of one surface with respect to the opposite one. We now investigate the effect of rotations. From the anisotropic nature of the self-affine surface, we have to distinguish between rotations around the z axis, normal to the mean fracture plane, and around an axis in the (x,y) plane. We will thus investigate these two kinds of rotations one after the other.

Let us first consider a rotation of angle ω_z around an

axis parallel to z, passing through the center of rotation $\Omega=(x_r,y_r,0)$. For any point M in the (x,y) plane, we can introduce the distance between the two surfaces at the point M

$$a(M)=z(M+\omega_z\vec{e}_z\times\overrightarrow{\Omega M})-z(M) . \quad (29)$$

If we call r the distance $r=\|\overrightarrow{\Omega M}\|$, two points which were initially facing each other are displaced by a distance $r\omega_z$. If we now combine the effect of a rotation and a translation parallel to the x axis, this simply corresponds to moving the center of rotation Ω.

We now restrict our discussion to the case where the projection of the surfaces in the (x,y) plane are disks of radius R and of center Ω. We can now reapply the same technique as above assuming $\omega_z \ll 2\pi$. We part the disk into boxes $S_i(r_i,\theta_i)$ whose size depends on the distance to the origin r_i. The shape of the boxes is defined in polar coordinates as limited by $\theta_i<\theta<\theta_{i+1}=\theta_i+\omega_z$ and $r_i<r<r_{i+1}=r_i(1+\omega_z)$. These boxes fulfill the same properties as in the case of translations. All boxes whose distance to the origin is r_i will contribute to an aperture $h_i\propto(r_i\omega_z)^\zeta$. Therefore the farthest boxes $r=R$ will be dominant. The number of boxes in the most distant annulus is simply $2\pi/\omega_z$. Thus we can adapt simply the result (24) to express the aperture for a rotation ω_z

$$h(\omega_z)\propto(R\omega_z)^\zeta\sqrt{1+K'\ln(2\pi/\omega_z)} . \quad (30)$$

If the boundaries of the surface in the (x,y) plane are different or if the center of rotation is different from the center of the disk, the above result can easily be extended, but the final result cannot be simply expressed in a closed expression for the general case.

Let us point out that Eq. (30) is obtained from Eq. (27) by replacing the sample size L by $2\pi R$ and the translation u by $R\omega_z$. This is equivalent to assuming that $h(\omega_x)$ is determined by the regions close to the sample rim where the displacement $r\omega_z$ is the largest; this is not surprising since, in the translation case, h increased monotonically with u. Then, the effective length over which the profile is sampled is $2\pi R$.

VI. ROTATIONS AROUND AN AXIS IN THE (x,y) PLANE

Let us now discuss the case of a rotation around an axis in the (x,y) plane. The interest of rotations whose axis lies in the (x,y) plane is not really to deal with a fixed prescribed rotation, but rather to address the more relevant situation where the upper surface is free to rotate. Then, a stable position of the upper surface will involve not one, but three (in three dimensions) points of contact. We can imagine that a first contact is created from a translation parallel to the z axis; then a rotation takes place around an axis going through the first contact point, until a second contact is created, and finally a last rotation takes place around an axis going through both contact points until a third contact is established such that the center of gravity of the upper block lies inside the triangle formed by the three contact points. If the last condition is not met, a new rotation is to be considered around two contacts, etc., until a stable position is reached. The question one may ask is whether or not this procedure affects significantly the previous results; this will allow one to determine whether the parallel motion procedure, which is much easier to implement both numerically and experimentally, yields results that are practically relevant.

The problem of rotations about an axis located in the (x,y) plane is very different from the previous case. Indeed, after a rotation of angle ω_y around the y axis, the surface is no longer self-affine in the (x,y,z) coordinate system. For a small angle ω_y, the surface is changed to $z(x,y)\rightarrow z(x,y)+\omega_y x$. The fact that the surface fluctuates can, however, hide this effect, but only at small scales. At large length scales, the bias induced by the rotation will become apparent in spite of the roughness. The crossover scale x^* along the x axis can be written as $\omega_y x^*=\sqrt{C(l)}(x^*/l)^\zeta$. Thus

$$x^*=\left[\frac{\sqrt{C(l)}}{\omega_y l^\zeta}\right]^{1/(1-\zeta)} . \quad (31)$$

If this rotation effect is considered together with a slip u along the x axis, we have to incorporate the effect of the rotation on the aperture function. As we have seen that the scale u corresponds to a change of regime, we have to consider two different cases.

(i) If x^* as defined above is smaller than u, the aperture can be considered as self-affine up to a scale x^*, and above this scale, the aperture will grow linearly with the distance x. For a surface limited by a square $0<x<L$ and $0<y<L$, the contact will be set first in the range $0<x<x^*$ and we will recover the result Eq. (28) with different constants.

(ii) If, on the contrary, the crossover scale x^* is larger than u as computed from Eq. (31), then one has to take into account the correlations in the aperture function [Eq. (21)] which do not depend on distance past u. The crossover is to be written $\omega_y x^*=\sqrt{C(l)}(u/l)^\zeta$ or

$$x^*=\left[\frac{\sqrt{C(l)}}{\omega_y l^\zeta}\right]u^\zeta . \quad (32)$$

The aperture will thus be self-affine with an exponent ζ up to a scale u. From u to x^*, the aperture will appear as uncorrelated and finally, above the scale x^*, it will increase linearly with distance. If the two surfaces are translated along z so as to establish a contact, the latter will most probably lie in the interval $0<x<x^*$.

A single contact does not provide a stable position for the upper block. Therefore, one may inquire about the effect of the further rotations which are needed to set these contacts. We investigate now the rotation produced by the establishment of contact between two complementary surfaces horizontally translated by a distance u. Let A_1 be the first contact point obtained after a translation parallel to z axis. A stable position requires three contact points. The second contact point A_2 is obtained after a rotation around an horizontal axis going through A_1. The second contact point is expected to be either very close $\|\overrightarrow{A_1A_2}\|<u\ll L$ or very far

$\|\overrightarrow{A_1A_2}\| \simeq L \gg u$ from A_1. The first case (i.e., $\|\overrightarrow{A_1A_2}\| \ll L$) results from the fact that the probability distribution $p(\|A_1A_2\|)$ to have a contact at distance $\|\overrightarrow{A_1A_2}\|$ is large in the immediate vicinity of 0, because A_1 is already a contact point and then the aperture is small close to A_1. As the distance $\|\overrightarrow{A_1A_2}\|$ increases up to the scale u the probability of contact decreases, but above u it rises again because the displacement due to the rotation is proportional to $\|\overrightarrow{A_1A_2}\|$, and hence results the second expectation (i.e., $\|\overrightarrow{A_1A_2}\| \simeq L \gg u$). In the case where $\|\overrightarrow{A_1A_2}\| \ll L$, the contact points (A_1, A_2) are most probably unstable because the orthogonal projection of the center of gravity of the upper surface has a small probability to lie within the distance $\|\overrightarrow{A_1A_2}\|$. The new contact A_2 thus will act as a new center of rotation, returning to the previous situation with A_2 instead of A_1.

We now focus our attention on the interesting case $\|\overrightarrow{A_1A_2}\| \gg u$ and estimate the rotation angle ω_c needed to reach the contact A_2. For a rotation of center $A_1(x_1,y_1)$ and axis y, we can describe the aperture between the two blocks as

$$d_u(x,y,\omega) = z(x,y) - z(x+u,y) - (x-x_1)\omega + h \ , \tag{33}$$

where h is the mean distance between the two surfaces. The angle ω_c can thus be written

$$\min_{x>0}(d_u(x,0) - \omega_c(x-x_1)) = 0 \ . \tag{34}$$

As previously done in Eq. (23), we partition the x axis in $u/L = n \gg 1$ adjacent boxes S_i of size u, such that $(i-1)u < x < iu$ for S_i and rewrite (30)

$$\begin{aligned} \omega_c &= \min_i \left[\min_{x \in S_i} \left[\frac{d_u(x,0)}{x - x_1} \right] \right] \\ &= \min_i(\omega_i) \ . \end{aligned} \tag{35}$$

There the set of values ω_i can again be considered as approximately independent variables. As in Eq. (25), numerical studies indicate a good agreement with a Gaussian probability distribution $\phi'(\omega_i)$ for ω_i. From the definition of ω_i given in Eq. (35) and the expression of d_u Eq. (33), (h/iu) and $(ku^{\zeta}/iu)^2$ are, respectively, the mean and the variance of the variable ω_i. Thus $\phi'(\omega_i)$ can be written

$$\phi'(\omega_i) \sim K \exp\left[-\left[\frac{(iu\omega_i - h)}{ku^{\zeta}} \right]^2 \right] . \tag{36}$$

Hence we can check that the probability for ω_c to reach a given value ω_c^* is

$$\begin{aligned} P(\omega_c > \omega_c^*) &= \prod_{i=1}^{i=n} \phi(\omega_i > \omega_c^*) \\ &= \prod_{i=1}^{i=n} \operatorname{erfc}\left[\frac{(iu\omega_c^* - h)}{ku^{\zeta}} \right] , \end{aligned} \tag{37}$$

where $\phi(\omega)$, the integral of $\phi'(\omega)$, is the complementary error function. In order to characterize ω_c^* we use the asymptotic behavior of $\phi(\omega_i)$, through the large argument expansion of the error function, since $(iu\omega_c^* - h)/ku^{\zeta}$ is large for $n \gg 1$ as checked afterwards. Considering the dominant term for large n, we obtain

$$P(\omega_c > \omega_c^*) = \exp\left[\frac{n^3 u^2 \omega_c^{*2}}{6k^2 u^{2\zeta}} [1 + O(n^{-1})] \right] . \tag{38}$$

A typical value (the median value) of ω_c^* is obtained for $P(\omega_c > \omega_c^*) = \frac{1}{2}$. A more complete analysis shows that a similar scaling is obtained for the average value

$$\omega_c^* = \sqrt{6\ln(2)} k \frac{u^{(\zeta+1/2)}}{L^{3/2}} [1 + O(n^{-1})] \ . \tag{39}$$

Let us now check that the previous hypothesis $(iu\omega_c^* - h)/ku^{\zeta} \ll 1$ is indeed satisfied. Let us first note that $iu\omega_c^*/ku^{\zeta}$ is bounded by $Lu\omega_c^*/ku^{\zeta}$, which can be estimated through Eq. (39) to be of order

$$\frac{L\omega_c^*}{ku^{\zeta}} \propto n^{-1/2} \ . \tag{40}$$

Therefore, we can simplify the expression to estimate $(iu\omega_c^* - h)/ku^{\zeta} \approx -h/ku^{\zeta}$, which is itself such that $\operatorname{erfc}(-h/ku^{\zeta}) \sim 1/n$. As a result, the asymptotic expression of the complementary error function used in the previous computation was legitimate.

Let us note that Eq. (40) has a simply physical meaning. The vertical displacement due to the rotation ω_c^* at a distance L of the contact point A_1 is small compared to the roughness of the surface. Therefore the rotation angle ω_c plays a minor role in the previous analysis of the vertical displacement of the blocks and can be neglected in the expression of the aperture. Therefore, the parallel displacements, which may have been considered as a drastic simplification of a realistic case, appear to induce the dominant effect. Additional rotations do not affect the validity of the expression of the aperture.

VII. NUMERICAL SIMULATIONS

Numerical simulations were performed to illustrate the previous analysis and to estimate the magnitude of the size effects given in Eq. (28). Moreover, this constitutes a partial check of the assumption that the Gaussian distribution of height differences gave rise to Gaussian distribution of apertures in elementary boxes S_i [Eqs. (25) and (35)]. In order to characterize this distribution we generated self-affine surfaces using a dichotomy algorithm introduced by Voss in Ref. [19]. We chose a roughness exponent equal to the experimental value (i.e., $\zeta = 0.83$). Figure 1 shows a typical surface generated by this method. We imposed a normalization such that the local roughness [i.e., $C(l)$] is kept constant and thus the overall roughness varies with the system size. Figure 3 gives the histograms of d_u obtained for different u parameters such that $u/L < 0.1$ for a system size $L = 1024$ (data collected over ten samples). The histograms have been rescaled following Eq. (24), in order to demonstrate the expected scale invariance. A Gaussian distribution parabola shows

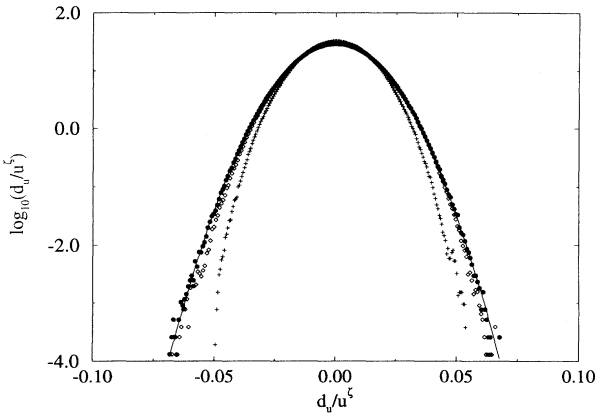

FIG. 3. Probability distribution of the rescaled height difference $d_u = |z(x,y) - z(x+u,y)|/u^\zeta$ obtained from numerical simulations for $L = 1024$ (data collected over ten samples) in a log-linear plot. The symbols are $\diamond$, $u = 8$; ●, $u = 32$; and +, $u = 64$: The continuous curve is a Gaussian fit for $u = 32$.

excellent agreement with the simulations in a similog plot. Numerical noise is smaller than point size. However, the data collapse for various u is not as perfect as could have been expected for artificially generated surfaces. This observation is consistent with a systematic study of size effects and measurement bias of self-affine measurements of Ref. [24]. We also checked numerically that the distribution p_2 of maxima h_i over the boxes as defined in Eq. (23) can be fitted to the scaling form similar to Eq. (24), with ϕ_2 having a Gaussian behavior for large and even moderate aperture.

Next, we checked the validity of the finite size effect predicted in Eq. (28) for the aperture $h(u)$ between two complementary surfaces horizontally translated by a distance u: $h(u) \propto u^\zeta \sqrt{1 + K' \ln(L/u)}$. Figure 4 shows in log-log coordinates the mean aperture $\langle h(u) \rangle$ averaged over 100 samples for different surface sizes L from 128 to 1024. For this computation, the overall roughness [hence $C(L)$ and to the small scale roughness $C(l)$] has been kept constant. As a result, all the curves have a common extreme point $u_{\max}/L = 0.1$ on the u/L axis. One can see that the aperture deviates strongly from the simple expectation $(u/L)\zeta$, indicated by a straight line. Moreover, as the system size increases, almost no change can be detected. This shows that one cannot use directly the aperture scaling in order to access to the self-affine properties of the surface. Figure 5 shows the finite size effect predicted in the previous sections. $[h(u)/u^\zeta]^2$ is plotted versus $\ln(u/L)$ for the same set of size L. Equation (28) predicts a linear relation between both quantities, which is seen to be closely followed. Deviations from the linear behavior are confined to displacements of the order of a few times the discretization length, so that for a given ratio u/L, larger profiles approach the straight line shown on Fig. 5.

VIII. FRACTURED ROCK SAMPLE AND PROFILOMETRY DATA

We have studied a parallelipedic block of granite with an initial size $25 \times 25 \times 15$ cm^3. Two parallel notches had been drawn in the middle of two opposite faces. The block has been fractured in two parts. The fracture surface is limited by the two notches. The size distribution of the geometrical features of the rough surface is very broad; their smallest dimension is of the order of a few micrometers, while their largest size extends over several centimeters.

We have first performed profilometry measurements along parallel straight segments on the fracture surface. The segment length is about 120 mm and the distance between neighboring profiles is 100 μm. The measurement is performed by lowering a detection tip until it touches the surface, recording the vertical contact position, and moving $\delta x = 48$ μm further horizontally to measure another point. The sensitivity of the technique is 5 μm and its repeatability is of the order of 10 μm. Ten such

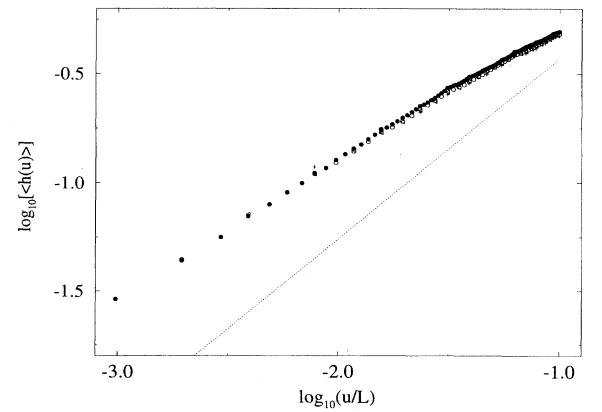

FIG. 4. Logarithm of the mean vertical displacement $\log_{10}[\langle h(u) \rangle]$ plotted vs $\log_{10}(u/L)$ for different surface sizes L (numerical simulations averaged over 100 samples). The symbols are +, $L = 128$; ◁ $L = 256$; ○, $L = 512$; and ●, $L = 1024$. The dotted line shows a power law of exponent $\zeta = 0.83$ for comparison.

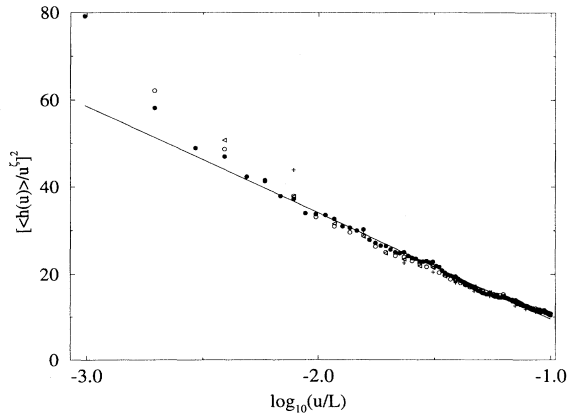

FIG. 5. Square of the rescaled mean vertical displacement $[\langle h(u) \rangle / u^\zeta]^2$ or self-affine surfaces of linear size L plotted versus the logarithm of the rescaled horizontal displacement $\log_{10}(u/L)$. The symbols are +, $L = 128$; ◁, $L = 256$; ○, $L = 512$, and ●, $L = 1024$. The straight line is a best fit to the data which represents the predicted behavior Eq. (28).

profiles $z(x)$ are displayed on Fig. 6. The clear correlation between the different profiles is a simple consequence of their proximity.

Figure 7 displays the averaged power spectrum pointed from the fast Fourier transforms of the ten profiles $z(x)$. In a log-log scale, the variation is linear over the whole range of wave vectors k investigated so that $P(k) \propto k^{-2.67}$. This result is in agreement with the assumption that the fracture surface is self-affine with a characteristic exponent $\zeta = 0.83$. Let us note that similar results have been obtained on various other crack surfaces [7]. Moreover, it is worth noting that the analysis of roughness profiles with a length of several meters measured along the faces of a granite fault inside a quarry [15] gave a very consistent estimate of the roughness exponent. This supports the suggestion that the results observed in our laboratory experiments can be transported to field measurements.

We also analyzed, from profilometry data, the $d_u(x) = z(x) - z(x+u)$ distribution used in Eqs. (25) and (36) and previously studied for numerically generated surfaces (see Fig. 8). Good agreement is shown with a Gaussian fit (in particular for $u = 16\delta x$), but extreme values of u seem to depart from such a behavior. Small u distributions display an exponential tail for large height differences. On the other hand, for large u values, the Gaussian distribution seems truncated. The latter effect may result from spurious sampling artifacts, but a proper understanding of this deviation remains to be clarified. Nevertheless, as shown below, this does not appear to result in significant deviations from the theoretically expected behavior of the aperture as a function of the displacement.

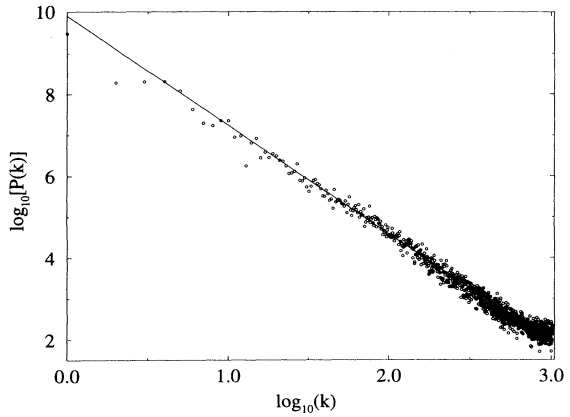

FIG. 7. Averaged power spectrum of the ten profiles plotted in log-log coordinates. A power law fit is shown on the graph with a slope $-1-2\zeta$, giving an estimate of $\zeta = 0.83 \pm 0.03$.

IX. EFFECTIVE APERTURE MEASUREMENT

We have analyzed the geometrical aperture of the crack in a well controlled way on the granite samples described above. We put the two fractured blocks in contact after having translated one block with respect to the other, keeping their orientations strictly parallel. We first start from the position at which the two blocks are at closest contact. This sets our origin for the relative displacements. Then, we study the vertical displacement $h(\delta x)$ for which the blocks are again in contact with a single contact point as a function of δx.

For that purpose, the upper block is held at a fixed position. The lateral displacement is limited within $\pm 10\ \mu$m by several ball point devices. Two detectors with a sensitivity of 5 μm allow one to control the lateral stability of the upper block. The vertical displacement of the upper block is limited downward by three horizontal stems resting on support plates. The height of the support plates is adjusted when the two blocks exactly coincide and is left fixed thereafter. Three vertical displacement detectors are located on the upper block near each of the three support stems. The lower block rests on three superimposed micropositioning devices controlling the displacement in the x, y, and z directions with a precision of 10 μm.

After the initial position of the lower block has been

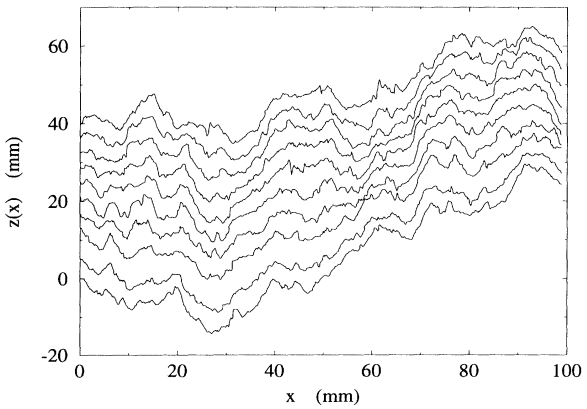

FIG. 6. Ten profiles measured on the granite rock fracture surface used in the experiments. The profiles have been collected along parallel lines close to each others so that the large scale roughness can be seen on different profiles. The profiles have been arbitrarily translated vertically for clarity.

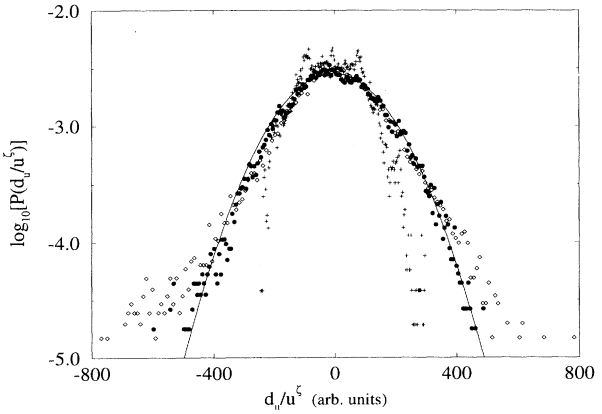

FIG. 8. Distribution of the rescaled height differences $d_u(x)/u^{\zeta} = |z(x) - z(x+u)|/u^{\zeta}$ from experimental profilometry data. Symbols are $\diamond$, $u = 4\delta x$; $\bullet$, $u = 16\delta x$; $+$, $u = 128\delta x$ with $\delta x = 48\ \mu$m. The continuous curve is a Gaussian fit to the $u = 16\delta x$ data.

adjusted, it is lowered and moved laterally in the x and/or y directions by a prescribed amount. Then, the block is raised until a motion is detected on *any one* of the three detectors. The corresponding z value corresponds to the first contact and is recorded before moving to another lateral position. A system of counterweights allows one to lower the force necessary to lift the upper block and to reduce the surface damage during the experiments. The horizontal displacements range from 0.1 to 25 mm and are increased a roughly geometrical progression. They have been performed in the four directions $\pm x$ and $\pm y$ in a systematic way and additional points have also been measured in other directions (e.g., 45° from x or the y axis).

X. EXPERIMENTAL OBSERVATIONS

We have estimated the repeatability of the experiments by superimposing experimental curves corresponding to a same direction of displacement. The data points are found to coincide within $\pm 20\ \mu$m.

We have overlayed on Fig. 9 four curves corresponding to four perpendicular directions of displacement $\pm x$ and $\pm y$. It is difficult to determine experimentally the origins $x=0$ and $y=0$ with an uncertainty better than about 100 μm since this contact corresponds to a minimum value of z around which its variation with x and y is small. We have therefore slightly adjusted the coordinates of the real origin with respect to our first initial determination so that the curves corresponding to variations along $\pm x$ and $\pm y$, respectively, coincide approximately at small distances. The adjustment was always smaller than 100 μm. This allowed us to obtain a very well defined relation between the aperture and the horizontal displacement, for *any orientation* of the displacement of the (x,y) plane, as can be seen on Fig. 9 where all four curves almost coincide over the whole range of variation of x and y.

This collapse of the data points onto a unique curve implies that the structure of the roughness is isotropic in the x-y plane, at least up to a distance of 25 mm, representing about one-tenth of the sample size. A second key point is the fact that the data points do not follow a simple power law. If a regression to a power law was performed on Fig. 9, in the upper range of u/L values, we would measure an apparent exponent less than 0.7, much smaller that the measured ζ exponent. This observation is quite consistent with the numerical simulations reported in Fig. 4. Thus the effect of the logarithmic term in Eq. (28) cannot be neglected if a quantitative analysis is to be performed.

In order to check Eq. (28), we have plotted in Fig. 10(a) the variations of the ratio $[h(u)/u^{\zeta}]^2$ as a function of the logarithm of the displacement $|u|$ parallel to the mean fracture surface. Figure 10(a) represents the variations obtained when the origin of the vertical displacement scale of the lower block corresponds to the closest contact observed experimentally. We observe, more precisely than in Fig. 9, that all four curves corresponding to different directions of displacement virtually coincide. We also observe that the linear decrease predicted by Eq. (28) is only obtained for $z > 200\ \mu$m.

However, experimentally, the determination of the origin (i.e., no relative displacement between the blocks) is

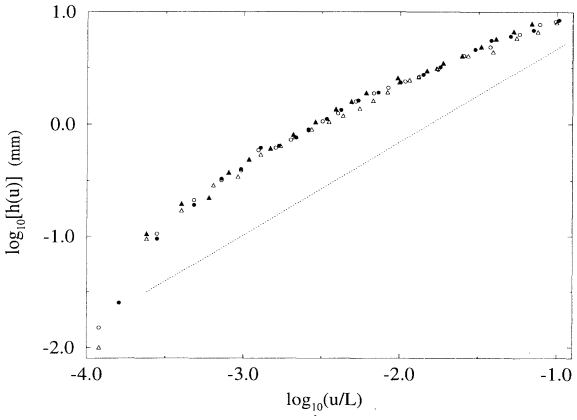

FIG. 9. Experimental measurement of the vertical displacement $h(u)$ as a function of the horizontal displacement u in four directions: Δ, $-x$; ▲, $+x$; ○, $-y$; and ●, $+y$. h is expressed in millimeters. A power-law of exponent $\zeta=0.83$ is drawn as a dotted line for comparison.

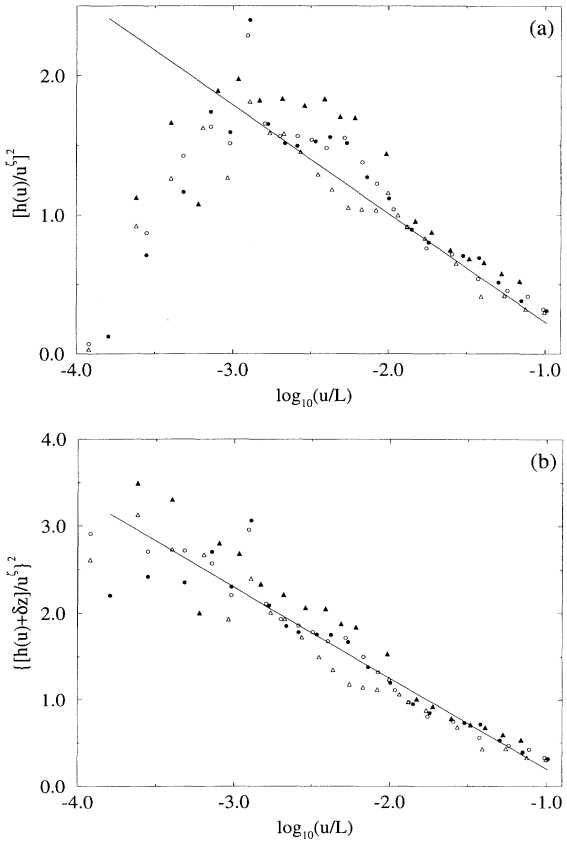

FIG. 10. Same data as Fig. 9 shown so as to test the prediction Eq. (28). u and h are expressed in millimeters. (a) The raw measured vertical displacement $h(u)$ is considered. (b) A vertical offset $\delta z = 80\ \mu$m (i.e., remanent aperture at closest contact) is taken into account.

never exact. We have already described the procedure followed to fix the origin of the positioning horizontally. Vertically, a perfect contact may be impossible if some irreversible deformation has taken place during the fracture process or if some small fragments are present on the surfaces. If we introduction a vertical offset δz, which corrects for this effect, and adjusts its value to $\delta z = 80$ μm, we observe a linear variation over the whole range of u values as shown in Fig. 10(b). The best fit drawn on this figure is, taking $L = 250$ mm,

$$h(u) + \delta z \propto u^{\zeta} \sqrt{1 + 1.67 \ln(L/u)} , \tag{41}$$

as shown in Fig. 10(b).

The value $\delta z = 80$ μm appears, however, to be large when compared to other observations of the fracture. Conductivity measurements to be reported elsewhere indicate that the remanant aperture at closets contact might be estimated to be $\delta z \approx 40$ μm. One should emphasize that a precise determination of this remanant aperture is extremely difficult because of the magnitude of the displacement involved and the varying sensitivities of different measurements. Moreover, the error bars on the aperture for small displacements u are quite large and thus extrapolating the fit in this region is to be considered with care.

In summary, the experimental results confirm clearly that the structure of the roughness is isotropic, at least up to length scales of the order of one-tenth of the sample size. The power spectrum of profiles varies as well defined power law $P(k) \propto k^{-1-2\zeta}$ of the wave vector k, which shows the self-affinity of the surface with a roughness exponent ζ comparable to reported values of the literature. The dependence of the fracture aperture on the relative horizontal displacement u between the two fractured blocks cannot be accounted for by a simple power law, but is accurately described by the previous theoretical analysis, which includes a slowly varying correction term.

XI. CONCLUSION

We have analyzed some properties related to the contact between two self-affine surfaces which are related to each other by a rigid body displacement. We have obtained analytical results which are supported by numerical simulations. These results lead to a closed expression for the geometrical aperture of cracks as a function of the relative displacement of the two sides.

The mere use of a scaling invariance thus appears to be a particularly rich and fruitful approach. Physical consequences of the problem studied here can be found in estimating the permeability and conductivity of a crack. This problem, of large importance in geophysical applications, is presently being investigated experimentally and has been considered in an earlier theoretical work [23].

Other applications can be considered in the field of the mechanical behavior of faults. Friction, wear, and gouge formation are also intimately related to an accurate description of the contact between rough surfaces. The present study shows that the use of a simple geometrical invariance of the crack roughness provides the necessary basis for deriving general but nontrivial results.

ACKNOWLEDGMENTS

We acknowledge the help of O. Pinet for the experimental measurements. We thank J. F. Legall and M. Ledoux for useful references. We also thank A. Hansen, H. J. Hermann, J. Koplick, K. J. Måløy, and J. P. Vilotte for useful discussions. We wish to thank O. Brouard and D. Vallet for the conception and realization of the experimental setup. This work has been supported by the Groupement de Recherche CNRS "Physique des Milieux Hétérogènes Complexes" and the ARC "Géochimie des Roches Chaudes et Séches." The "Laboratoire de Physique et Mécanique des Milieux Hétérogènes" is "Unité de Recherche Associée au CNRS" No. 857. The "Laboratoire de Géologie" is "Unité de Recherche Associée au CNRS" No. 1316.

[1] K. J. Evans, T. Kohl, R. J. Hopkirk, and L. Rybach, NEFF Project No. 359 (unpublished).
[2] See, e.g., C. C. Barton and E. Larsen (unpublished).
[3] B. Ledésert, J. Dubois, A. Genter, and A. Meunier, J. Volc. Geoth. Res. **57**, 1 (1993).
[4] E. Charlaix, E. Guyon, and R. Roux, Transp. Por. Med. **2**, 31 (1987).
[5] I. Ippolito, G. Daccord, P. Kurowski, and J. P. Hulin (unpublished).
[6] P. A. Witherspoon, Geo. Res. Lett. **8**, 659 (1981).
[7] S. R. Brown, J. Geophys. Res. **92**, 337 (1987); **94**, 429 (1989); Geophys. Res. Lett. **13**, 1430 (1986).
[8] R. Gutfreund and A. Hansen (unpublished).
[9] J. Feder, *Fractals* (Springer, New York, 1990).
[10] B. B. Mandelbrot, D. E. Passoja, and A. J. Paullay, Nature **308**, 721 (1984).
[11] R. H. Dauskardt, F. Haubensak, and R. O. Ritchie, Acta Metall. Mater. **38**, 143 (1990).
[12] B. L. Cos and j. S. Y. Wang, Fractals **1**, 87 (1993).
[13] P. Meakin, Phys. Rep. **235**, 189 (1993).
[14] E. Bouchaud, G. Lapasset, and J. Planès, Europhys. Lett. **13**, 73 (1990); K. J. Måløy, A. Hansen, E. L. Hinrichsen, and S. Roux, Phys. Rev. Lett. **68**, 213 (1992).
[15] J. Schmittbuhl, S. Gentier, and S. Roux, Geophys. Res. Lett. **20**, 639 (1993).
[16] N. Barton, in *Scale Effects in Rock Masses,* edited by A. Pinto da Cunha (Baklema, Rotterdam, 1990), p. 31.
[17] A. Chudnovsky and B. Kunin, J. Appl. Phys. **62**, 4124 (1987); A. Hansen, C. Poirier, K. J. Måløy, D. Bideau, and S. Roux (unpublished).
[18] J. Schmittbuhl, F. Schmitt, and C. Sholtz (unpublished).
[19] R. F. Voss, in *Fundamental Algorithms in Computer Graphics,* edited by R. A. Earnshaw (Springer-Verlag, Berlin, 1985), pp. 805–835.
[20] P. Lévy, *Processus Stochastiques et Mouvement Brownien* (Gauthier-Villar, Paris, 1948).
[21] M. Talagrand, Ann. Ins. Henri Poincaré **24**, 307 (1988).
[22] E. J. Gumbels, *Statistics of Extremes* (Columbia University Press, New York, 1958).
[23] S. Roux, J. Schmittbuhl, J. P. Vilotte, and A. Hansen, Europhys. Lett. **23**, 277 (1993).
[24] J. Schmittbuhl, J. P. Vilotte, and S. Roux, Phys. Rev. E (to be published).